

## <sup>1</sup>H HRMAS NMR Spectroscopy and Chemometrics for Evaluation of Metabolic Changes in *Citrus sinensis* Caused by *Xanthomonas axonopodis* pv. *citri*

Lorena M. A. Silva,<sup>a</sup> Elenilson G. Alves Filho,<sup>a</sup> Rafael Choze,<sup>a</sup> Luciano M. Lião<sup>a</sup> and Glaucia B. Alcantara<sup>\*,a,b</sup>

<sup>a</sup>Laboratório de Ressonância Magnética Nuclear, Instituto de Química, Universidade Federal de Goiás, CP 131, 74001-970 Goiânia-GO, Brazil

<sup>b</sup>Departamento de Química, Centro de Ciências Exatas e Tecnologia, Universidade Federal de Mato Grosso do Sul, CP 549, 79074-460 Campo Grande-MS, Brazil

A bactéria *Xanthomonas axonopodis* (*Xac*) causa uma das mais temidas e incuráveis doenças da citricultura: o cancro cítrico. Para compreender o mecanismo de resposta das laranjeiras quando atacadas pela *Xac*, folhas e frutos de *Citrus sinensis* foram diretamente avaliados por espectroscopia de RMN HRMAS (ressonância magnética nuclear de alta resolução com giro no ângulo mágico). Esta técnica permite a análise de amostras sem as laboriosas etapas de pré-tratamento, acessando as informações importantes sobre a sua composição química. As folhas de laranjeira e cascas do fruto investigadas neste estudo demonstraram as alterações bioquímicas causadas pela *Xac*. Auxiliado pelas análises quimiométricas, os resultados de RMN HRMAS apresentaram alterações relevantes no conteúdo de aminoácidos, carboidratos, ácidos orgânicos e terpenóides.

*Xanthomonas axonopodis* (*Xac*) bacterium causes one of the most feared and untreatable diseases in citriculture: citrus canker. To understand the response mechanisms of orange trees when attacked by *Xac*, leaves and fruits of *Citrus sinensis* were directly evaluated by HRMAS NMR (high resolution magic angle spinning nuclear magnetic resonance) spectroscopy. This technique allows the analysis of samples without laborious pre-treatments and also allows access to important information about chemical composition of samples. The orange tree leaves and fruit peels investigated in this study demonstrated the biochemical changes caused by *Xac*. Aided by chemometric analysis, the HRMAS NMR results show relevant changes in amino acids, carbohydrates, organic acids and terpenoids content.

**Keywords:** <sup>1</sup>H HRMAS NMR, citrus canker, *Citrus*, *Xanthomonas axonopodis*, metabolic fingerprint, chemometrics

### Introduction

Citriculture plays a role of great importance in the Brazilian economy because Brazil is the largest citrus producer in the world.<sup>1</sup> However, Brazil's competitive capacity has shown instabilities with the introduction of plant health problems, such as citrus canker, which lead to rising production costs.

Citrus canker is one of the most aggressive and feared disease that afflicts several *Citrus* species, and it is caused by the *Xanthomonas axonopodis* pv. *citri* (*Xac*) bacterium.<sup>2</sup> The disease has occurred in islands of the Indian Ocean, in the Middle East and in North America.<sup>2</sup> In Brazil, citrus

canker is occasionally present in some major producer states.<sup>3,4</sup>

Recent studies have been carried out with the aim of obtaining an efficient bactericide against citrus canker. For over one hundred years, copper compounds have been adopted to fight bacteria and fungi,<sup>5</sup> but the *Xac* bacterium has been shown to be resistant to such treatments.<sup>6</sup> The combination of a group of ethylene-bis-dithiocarbamate fungicides mixed with copper compounds and sanitary pruning have been reported as alternatives to fight citrus canker.<sup>7,8</sup> Nevertheless, the only effective way to eliminate this disease is by eradication of the plant and eliminating sprouts beyond the temporary interdiction of the cultivated area.<sup>9</sup> Hence, studies aimed at understanding the chemistry of citrus canker manifestations and the possible mechanisms

\*e-mail: glaucia.alcantara@ufms.br

of bacterial stress response are significant in combating this disease.

Nuclear magnetic resonance (NMR) is an important analytical tool for complex mixture analysis, such as in the quality control of food, analysis of metabolites from plants and animals, chemotaxonomic classification of species and industrial product analysis.<sup>10-13</sup> NMR provides, in particular, the appropriate technology and sufficient resources to enable reproducible analysis for molecular identification and quantification. Moreover, NMR has been a technique of great relevance in studies concerning plant defense mechanisms through structural proteomics by allowing for structure determination and the elucidation of structure-function relationships.<sup>14</sup>

In this context, the high resolution magic angle spinning (HRMAS) technique provides the advantages of solution and solid-state NMR, allowing for the combination of the most important characteristics of both techniques, such as the high resolution obtained by solution NMR and the minimal necessity for sample preparation inherent to solid NMR.<sup>15</sup> Additionally, *in natura* samples can be analyzed via NMR. HRMAS has also demonstrated high sensitivity in detecting mixture components at concentrations of up to  $1 \mu\text{mol L}^{-1}$ , and only requires a few minutes to obtain the results for the  $^1\text{H}$  nucleus.<sup>16,17</sup>

Considering the fact that NMR data have generated highly complex matrices with a large inherent spectral similarity, visual analysis may be unfeasible. Therefore, chemometrics can be adopted to employ statistical, mathematical and computational tools in the chemical data treatment and for the interpretation of multivariate data.<sup>18</sup> For this purpose, exploratory methods can be applied to NMR data, such as principal component analysis (PCA) and hierarchical cluster analysis (HCA).

Thus, this work aimed to evaluate the metabolic changes caused by citrus canker in *Citrus sinensis* (leaves and fruit peels) by  $^1\text{H}$  HRMAS NMR combined with chemometrics. The study of the response mechanism of *Citrus sinensis* attacked by *Xanthomonas axonopodis* provides an interesting basis for understanding the action of this pathogen.

## Experimental

### Plant material and preparation

Healthy and citrus-canker-contaminated leaves and fruits were obtained from two different orange trees [*Citrus sinensis* (L.) Osbeck, var. caipira], located in Vicentina City, Mato Grosso do Sul State, Brazil, collected through random sampling and maintained at low temperature ( $-21^\circ\text{C}$ ) until the sample preparation for NMR analyses.

For sample preparation, twelve healthy leaves and the same amount of citrus-canker-contaminated leaves were selected. The orange peels were removed from each three healthy and diseased fruits. From each diseased leaves and peels, the visible lesions of citrus canker were separated originating two new batches: diseased samples without citrus canker lesions and diseased samples with only the citrus canker lesions. After these, the resultant three types of leaves and orange peels (healthy samples, diseased samples without citrus canker lesions and diseased samples with only the citrus canker lesions), as shown in Figure 1a, were separately powdered using liquid nitrogen and about 2.5 mg were inserted in the HRMAS rotor, adding two  $\text{D}_2\text{O}$  drops. In Figure 1b, an example of a diseased leaf sample with and without lesions is highlighted.

### HRMAS NMR measurements

$^1\text{H}$  NMR spectra were recorded on a Bruker Avance III 500 (11.75 T) spectrometer operating at 500.13 MHz ( $^1\text{H}$ ) and equipped with a 4-mm HRMAS probehead,  $^1\text{H}$  and  $^{13}\text{C}/^{31}\text{P}$  and magnetic field gradient coils. A few drops of  $\text{D}_2\text{O}$  were added to the samples to obtain a lock and to adjust the local field homogeneity. The internal standard (3-trimethylsilyl)-2,2',3,3'-tetradeuteropropionic acid (TMSP- $d_4$ ;  $1 \text{ mg mL}^{-1}$ ) was used for calibration and signal quality assessment. Samples were placed into  $12 \mu\text{L}$  zirconia rotors with a teflon spacer to provide a spherical volume for the material.

For data optimization, a diseased orange peel without citrus canker lesions was used. The spectra were acquired from two different pulse sequences (with water signal suppression): composite pulse presaturation (CPPR) and Carr-Purcell-Meiboom-Gill (CPMG), using 300 ms as the total spin-spin relaxation delay ( $2n\tau$ ). Each experiment was acquired with 5 kHz of rotor spinning at the magic angle ( $54.74^\circ$ ). Typically, 128 free induction decays (FID) were collected into 32 K data points for 8012.820 Hz of spectral width with a relaxation delay of 2 s and an acquisition time of 2.05 s. Spectral processing was performed with 64 K points and line broadening (used to exponential multiplication) equal to 0.3 Hz.

Considering the fact that CPMG did not improve the spectral quality, it was not chosen as the method for spectral acquisition. After experimental optimization, three spectra were recorded from three different packing in HRMAS rotor resulting in a total of nine replicates using the CPPR sequence with the parameters described above. Correlation spectroscopy (COSY) and gradient-selected heteronuclear single quantum coherence (gHSQC) were used to provide information about the compounds present in the samples.

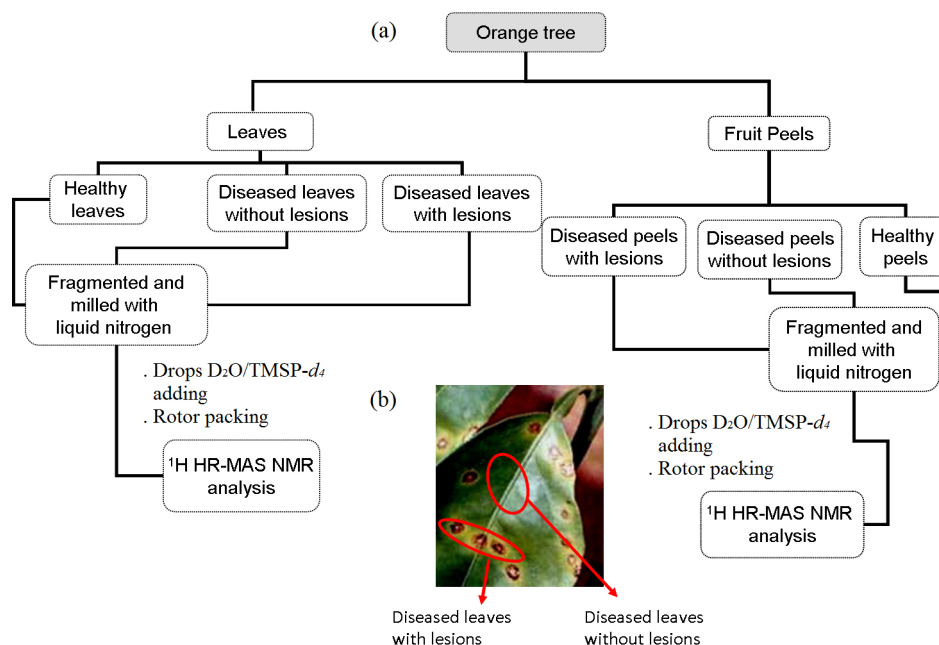


**Figure 1.** (a) Sample preparation schemes for <sup>1</sup>H HRMAS NMR analyses and (b) designation of diseased leaf samples with and without citrus canker lesions.

After analysis, all samples and materials were autoclaved to eliminate the bacteria.

#### Chemometric treatment

All spectral data were converted to American Standard Code for Information Interchange (ASCII) files and exported to the Pirouette<sup>®</sup> 4.0 program (Infometrix, Inc., Bothell, WA) for chemometric analysis. Each processed point in chemometric matrices corresponded to 0.12 Hz (bucket width).

Before the application of the chemometric algorithms, the spectral regions containing only noise (from  $\delta$  5.32 to 6.41 and above  $\delta$  8.29 for leaves;  $\delta$  5.44 to 6.11 and above  $\delta$  8.20 for peels), TMSP (below  $\delta$  0.78 and 0.61 for leaves and peels, respectively) and D<sub>2</sub>O resonance and its surrounding ( $\delta$  4.56 to 5.06 and  $\delta$  4.39 to 5.05 for leaves and peels, respectively) were removed.

Principal component analysis (PCA) and hierarchical cluster analysis (HCA) methods were performed to understand the metabolic variation induced by citrus canker.

PCA was performed with autoscaled preprocessing (mean centered and scaled to unit variance), which assigns the same loading to variables. Normalize scaling parameter and baseline correction using linear fit algorithms were applied to reduce the differences in concentration and sample noise. For HCA, the matrices were also autoscaled, normalized and baseline corrected, and the incremental linkage method (sum-of-squares approach in calculating intercluster distances) was applied.

## Results

### Spectral overview of the samples

<sup>1</sup>H HRMAS NMR spectra of the vegetal material showed signals from the main primary metabolites, in particular carbohydrates and amino acids. Spectra for both group of samples (leaves and peels) showed three different regions: aromatic hydrogen ( $\delta$  6.0 to 9.0), carbinolic hydrogen ( $\delta$  3.0 to 6.0) and  $\alpha$ -carbonylic/alkyl residue hydrogens ( $\delta$  1.0 to 3.0).

According to literature,<sup>19,20</sup> in comparison to 2D NMR experiments, <sup>1</sup>H HRMAS NMR assignments of healthy orange tree leaves showed the presence of leucine, valine, treonine, alanine, proline, glutamine/glutamic acid, citric acid, malic acid, succinic acid, aspartate,  $\gamma$ -aminobutyric acid (GABA), tryptophan, tyrosine and  $\alpha$ - and  $\beta$ -glucose carbohydrates (Figure 2a). Diseased leaves showed changes in some of these metabolites, essentially the reduction in carbohydrate content (Figures 2b and 2c).

For healthy orange peels, <sup>1</sup>H HRMAS NMR spectra showed resonances of limonene, glutamine/glutamic acid, citric acid, malic acid, succinic acid, aspartate, tryptophan and tyrosine, as well as  $\alpha$ - and  $\beta$ -glucose and sucrose carbohydrates (Figure 3a). In diseased peels, limonene and carbohydrates signals were visually reduced (Figures 3b and 3c).

Although NMR spectra have shown an expressive change in the proportion of some compounds when orange leaves and peels were infected by citrus canker, the aid

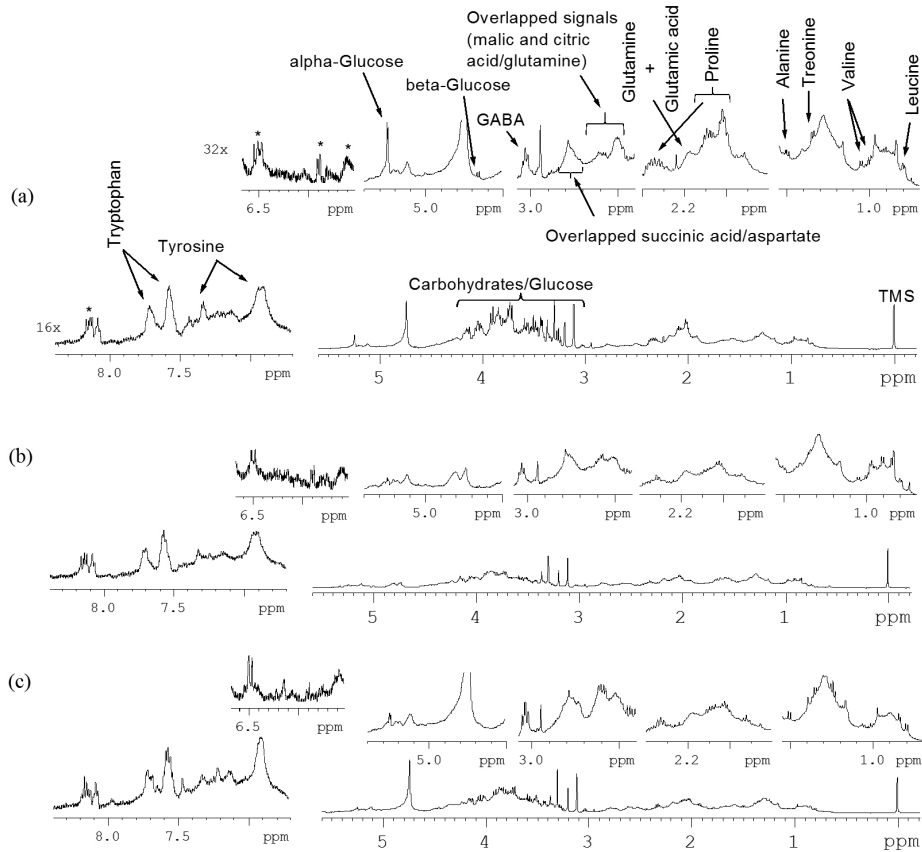


**Figure 2.** Representative spectral profile of  $^1\text{H}$  HRMAS NMR from orange tree leaves: (a) healthy samples, (b) diseased samples without *Xac* lesions and (c) diseased samples with *Xac* lesions. \*Unknown compounds.

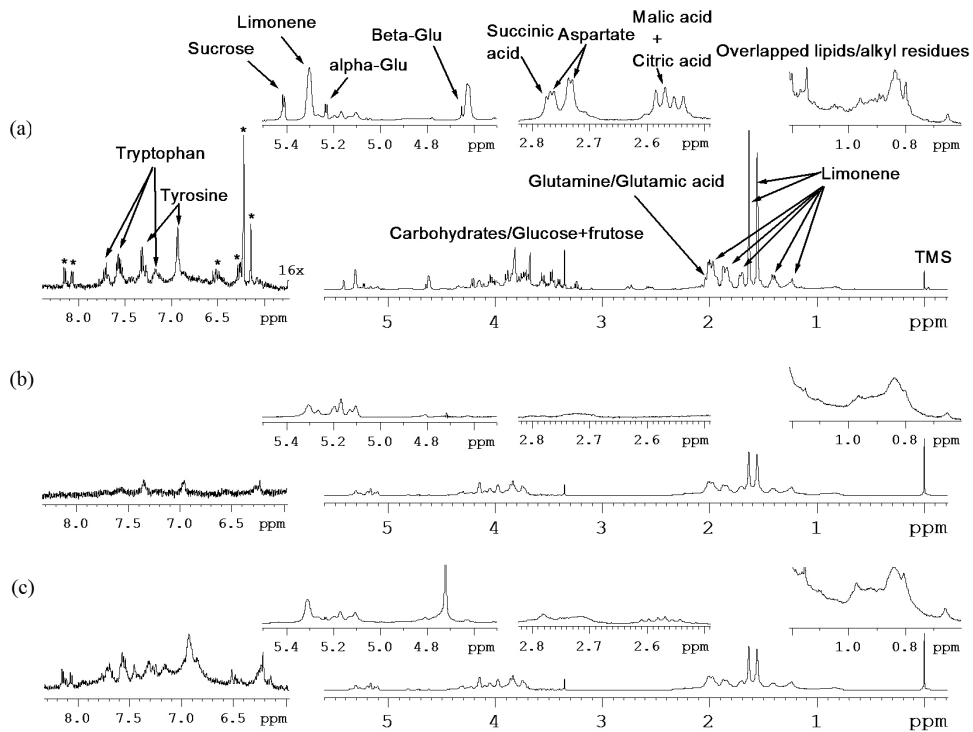


**Figure 3.** Representative spectral profile of  $^1\text{H}$  HRMAS NMR from orange peels: (a) healthy samples, (b) diseased samples without *Xac* lesions and (c) diseased samples with *Xac* lesions. \*Unknown compounds.

of chemometrics has become essential to analyze the influence of each compound variation and to detect some imperceptible metabolic changes.

#### Assessment of orange tree leaves

Initially, it was applied the unsupervised agglomerative method (HCA), which groups natural clusters into a two-dimensional space (dendrogram). In the dendrogram of orange tree leaves (Figure 4a), the samples were set according to their proximity represented by Euclidean distance using the incremental linkage method. Groups were formed by the closest samples (similar) at a similarity index near 1 and distant samples (different) at a similarity index near zero.<sup>21</sup>

Two important clusters could be observed, with the first (I) featuring healthy orange tree leaves and the second (II) featuring diseased leaves, reflecting the natural differences between sample groups, which are formed as a

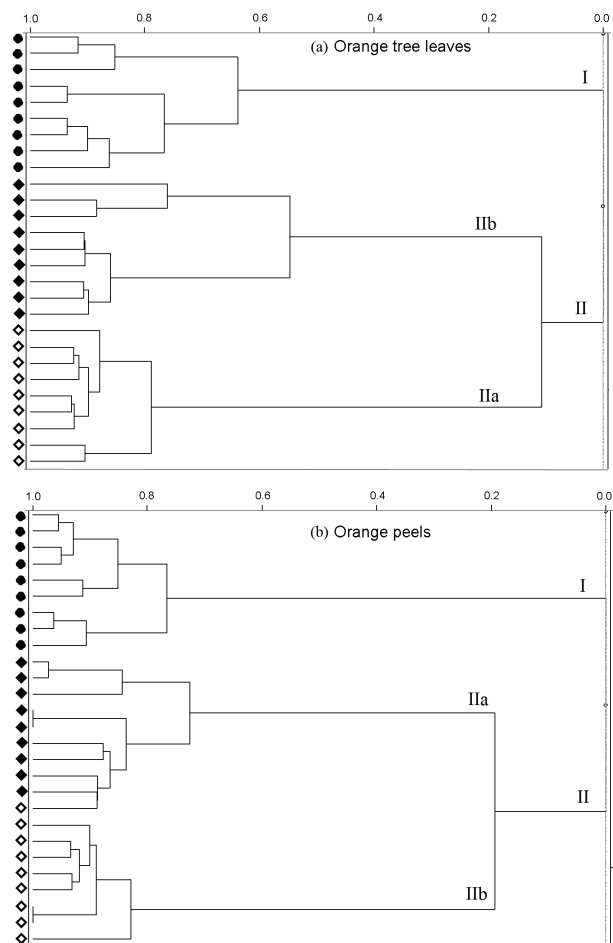


**Figure 4.** Dendrograms from (a) orange tree leaves and (b) orange peels directly analyzed by  $^1\text{H}$  HRMAS NMR. Legend: healthy samples (●), diseased samples without lesions (◆) and diseased samples with lesions (◇).

function of pathogenic conditions, independent of the degree of pathogen incidence. On the other hand, with a similarity index of 0.11, the second group (II) was subdivided into diseased leaves without lesions (IIa) and those containing lesions (IIb), according to the disease level incidence.

To reduce the dimensionality of the original data and to assist the modeling and interpretation of multivariate data, PCA was applied. The grouping observed in HCA was very important in interpreting the score plot obtained via PCA (Figure 5a), which exhibits a clear sample separation with respect to PC1 and PC2, with a total variance of 74.5%.

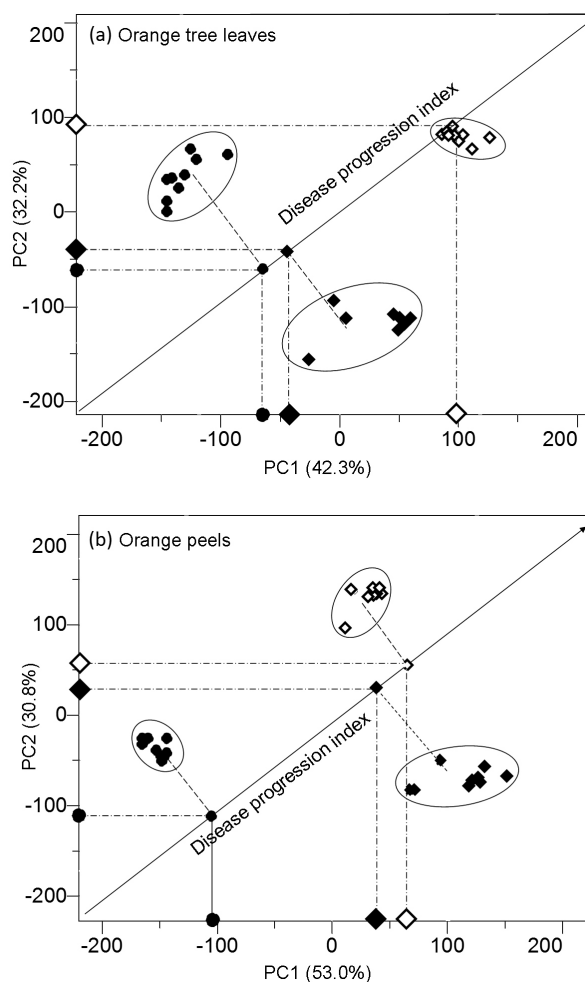


**Figure 5.** PCA score plots of  $^1\text{H}$  HRMAS NMR spectra from (a) orange tree leaves and (b) orange peels. Legend: healthy samples (●), diseased samples without lesions (◆) and diseased samples with lesions (◇).

In PCA, groups from HCA dendrogram were displayed when a bisector of the factorial axes was drawn. Perpendicular projections of the samples under the bisector indicated the disease progression from positive PC1 and PC2 scores. In both axes, the sequence of disease incidence was observed on the positive scores and was interpreted as an index of biochemical changes in function of the

pathogen. Healthy and diseased leaves without lesions were more similar, and diseased leaves with lesions were more different from the other samples, indicating that the biochemical changes were more expressive when the lesions are present.

To understand the mechanism of infection and the compounds responsible for biochemical changes in PC1, the loading plot (Figure 6a) suggests that the  $^1\text{H}$  NMR regions about at  $\delta$  1.1-1.6 (valine, treonine, alanine and overlapped compounds such as lipids),  $\delta$  2.3-3.0 (proline, glutamic acid/glutamine, malic, citric and succinic acids, aspartate and GABA) and  $\delta$  6.8-8.2 (tryptophan, tyrosine and unknown compounds) were responsible for disease incidence in samples in the positive scores of PC1. NMR signals at  $\delta$  1.8-2.1 and 2.3 (proline),  $\delta$  3.0-4.2 (carbohydrates) and  $\delta$  5.22 ( $\alpha$ -glucose) determined the presence of healthy samples in the negative scores of PC1.

On PC2 loadings (Figure 6a), NMR regions at  $\delta$  2.6-2.9 (aspartate and succinic acid),  $\delta$  3.2-4.5 (carbohydrates),

$\delta$  5.0-5.4 ( $\alpha$ -glucose and sucrose) and  $\delta$  6.5-6.7 (unknown compounds) induced the axis composition in the more positive scores of PC2, allocating diseased leaves with lesions on positive PC2. The regions at  $\delta$  0.8-1.25 (leucine and lipids),  $\delta$  1.8-2.1 and  $\delta$  2.3 (proline),  $\delta$  2.5-2.7 (glutamine, malic, citric and succinic acids and aspartate) and  $\delta$  8.1-8.2 (unknown compounds) were responsible to negative loadings of PC2, allocating diseased leaves without lesions on negative PC2.

Beyond some compounds above cited in which the spectral variation was not obvious, carbohydrate and proline signals were dramatically reduced in diseased leaves, especially before the eruption of *Xac* lesions. The GABA content seemed similar in healthy and diseased leaves with lesions and was evidently decreased in diseased leaves without lesions. The consumption of these metabolites in diseased leaves before *Xac* lesions was expressed as a stress response at the expense of the preservation and/or production of other compounds.

#### Assessment of orange peels

In the orange peel analyses, to determine the general structure of the data, HCA was also performed (Figure 4b). The resultant dendrogram was very similar to that obtained from the orange tree leaves, showing first the separation between healthy (I) and diseased (II) orange peels, and from similarity index of 0.20, the group of diseased orange peels (II) was subdivided into diseased peels without lesions (IIa) and those containing lesions (IIb), according to the disease level incidence (Figure 2b).

In PCA, which described 85.2% of the total variance, the index of disease progression was also manifested by a bisector from positive scores of PC1 and PC2, and by the projections on the factorial axes (Figure 5b). On PC1, healthy and diseased samples are separated, but diseased samples with and without lesions are not satisfactorily separated. On PC2, a separation is clearly observed for samples with and without lesions. Therefore, the differences between healthy and diseased samples on PC1 may be due to the metabolic response of the plant to infestation (independent of lesions), and on PC2, a separation observed for samples with and without lesions is due to the metabolic changes caused by lesions. Thus, both axes represent biochemical changes, one caused by infection in general and the other caused by occurrence of lesions.

An assessment of the loading plot (Figure 6b) was performed and the regions from  $\delta$  0.8-2.5 (limonene and overlapped lipids/alkyl residues),  $\delta$  3.8-4.2 (carbohydrates),  $\delta$  5.1-5.4 ( $\alpha$ -glucose and sucrose) and  $\delta$  6.2-8.2 (tryptophan,

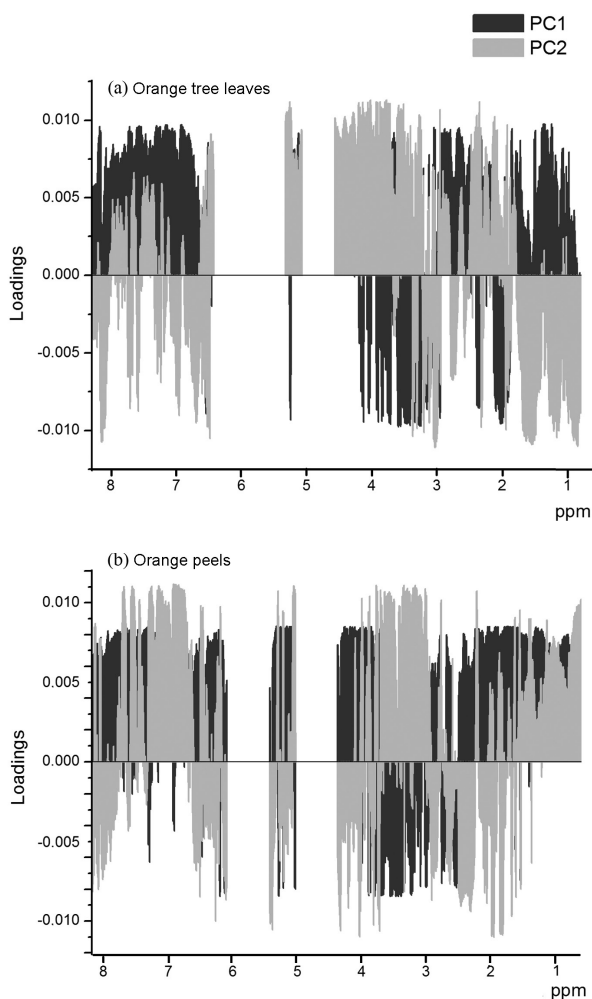


**Figure 6.** PCA loading plots of  $^1\text{H}$  HRMAS NMR spectra from (a) orange tree leaves and (B) orange peels.

tyrosin and unknown compounds) were identified as being responsible for the distribution of the diseased samples in the positive scores of PC1. The regions around  $\delta$  2.5 (citric and malic acids),  $\delta$  2.7 (aspartate and succinic acid) and  $\delta$  3.9-4.4 (carbohydrates) contributed to the determination of healthy orange peel samples in the negative scores of PC1.

Considering the fact that in HRMAS the sample undergoes a minimal pre-treatment, the region from  $\delta$  0.8 to 2.5 attributed to limonene and overlapped lipids/alkyl residues, such as essential oil residues, could be visualized and was relevant to discriminate healthy and diseased orange peels, independently of the infection level, because the reduction of limonene was observed as a stress response in bacterial infection sites.

According to Figure 3, a clear reduction in  $\alpha$ -glucose,  $\beta$ -glucose and sucrose content can be observed when the leaves are infected by citrus canker. Likewise, aspartate and succinic, citric and malic acids were reduced after the pathogen incidence. Therefore, PCA corroborated the separation between healthy and diseased orange peels on the PC1 axis induced by these loadings (Figure 6b).

From PC2 loadings (Figure 6b), the production of compounds at  $\delta$  0.8 (overlapped lipids/alkyl residues),  $\delta$  3.0-4.0 (carbohydrates) and  $\delta$  5.2 ( $\alpha$ -glucose) was almost ceased with bacterial incidence and these NMR signals were responsible for allocating the diseased orange peel samples with lesions in the positive scores of PC2.

Regions from  $\delta$  1.8-1.9 (lipids/alkyl residues) and  $\delta$  4.0, 4.3 and 5.4 (sucrose) in <sup>1</sup>H HRMAS NMR spectra were responsible for allocating the diseased orange peel samples without lesions in the negative scores of PC2, separating diseased orange peels before and after the eruptions of *Xac* lesions.

## Discussion

NMR spectroscopy was successfully used to investigate metabolites from orange matrices affected by the *Xac* bacterium, indicating the high efficiency of the exploratory analysis of monitoring.

From orange tree leaves and peels, the sequence of disease incidence of the bisector on PC1 and PC2 axes was interpreted as an index of biochemical changes in function of the pathogen.

In evaluation of orange tree leaves, amino acids, such as alanine, treonine, leucine, valine and GABA, beyond organic acids were classified as important compounds for metabolic variation (Figures 2 and 6a). These amino acids, especially the increment of GABA, are related to a response against pathogens due to the fact that there was resistance

induction against certain pathogens in plants when samples were treated with some amino acids.<sup>22,23</sup>

However, considering the fact that bacterial cell walls contain macromolecules such as carbohydrates, lipids and proteins,<sup>24</sup> which exhibit aliphatic chain <sup>1</sup>H NMR signals of about  $\delta$  1.0 to 3.0,<sup>25</sup> additional experiments were performed using isolated *Xac* (Figure S1 in the Supplementary Information section), corroborating that all of the compounds assessed were produced by orange trees at the site of *Xac* eruption.

In orange peels, the reduction of the limonene content (Figures 3) suggests that the plant uses this antimicrobial compound as a defense mechanism against *Xac*. The fact that essential oils responsible for taste, smell and food conservation,<sup>26</sup> besides exerting antimicrobial activities,<sup>27</sup> are reduced at bacterial infection sites indicates the attempt of the plant to combat *Xac* bacteria. However, the consumption of limonene causes the loss of microbial activity, which renders a plant even more vulnerable to citrus canker.

According to the literature,<sup>28,29</sup> *Xac* induces gene transcription related to resistance, defense and response to pathological stress induced by alkaloids, terpenes and volatile compound production. However, during lesion development, there is a suppression of the defensive responses and the mobilization of nutrients toward infection sites. Hence, in orange peels, limonene has been responsible for PC1 characterization, and the compound variability justifies the distribution observed in the PCA.

Corroborating the results showed in leaves, the reduction of citric, malic and succinic acids and aspartate (compounds between  $\delta$  2.4 and 3.0) suggested the pathogen incidence in orange peel samples.

Changes in carbohydrate content, such as  $\alpha$ - and  $\beta$ -glucose, and sucrose was also observed in leaf orange peel samples (Figure 2 and 3). It is known that *Xac* decreases biosynthetic rates<sup>30</sup> and protein catabolism,<sup>28</sup> whereas carbohydrates are considered signals of metabolism regulation, development and stress response.<sup>31,32</sup> Moreover, the production of these compounds was practically stopped with infection, which may be associated with the supply of energy required for metabolism reactions important for defense mechanisms. Therefore, PC1 expressed the biochemical change index mainly represented by carbohydrate catabolism before morphological changes. Furthermore, a prediction model for canker infestation in *Citrus* based on carbohydrate catabolism could prove useful by signaling a total reduction in carbohydrate production when a plant is affected by citric canker disease.

## Conclusion

The biochemical changes in orange tree leaves and fruit peels reveal the defensive metabolism of *Citrus sinensis* against citrus canker. NMR spectral regions highlighted by the PCA loadings confirm similar results between orange tree leaves and fruit peels. There was mainly a variation in the amino acids, organic acids and carbohydrate signals, corroborating the presence of carbohydrates as a signal of metabolism. The decrease observed for these metabolites in diseased plants represents the plant response to the stress caused by *Xac*, having the potential to trigger the expression of apoptosis, a process of programmed cell death used to avoid the disease advance. Moreover, changes in essential oils were responsible for PCA variability in orange peels because HRMAS analysis samples underwent a minimum pre-treatment and thus their compounds could be analyzed.

Understanding the action of this pathogen could allow for the designing of new tools to prevent or combat *Xac* infection, especially before the morphological changes.

## Supplementary Information

Supplementary data (comparative spectral profile of <sup>1</sup>H HRMAS NMR from isolated *Xac* and orange tree leaves with lesions caused by *Xac*) are available free of charge at <http://jbcbs.sbg.org.br> as a PDF file.

## Acknowledgements

We thank Conselho Nacional de Desenvolvimento Científico e Tecnológico (CNPq), Coordenação de Aperfeiçoamento de Pessoal de Nível Superior (CAPES) and Financiadora de Estudos e Projetos (FINEP) for their financial support.

## References

1. <http://www.fao.org> accessed in July 2009.
2. CABI and EPPO. In *Quarantine Pests for Europe*; ed. CABI Publishing, Wellingford, Oxford, UK, 1997, 2, 1101.
3. Civerolo, E. L.; *J. Rio Grande Val. Hortic. Soc.* **1984**, 37, 127.
4. Massari, C. A.; Belasque Jr., J.; *Citrus Res. Technol.* **2006**, 27, 41.
5. Nakajima, M.; Goto, M.; Hibi, T.; *J. Gen. Plant Pathol.* **2002**, 68, 68.
6. Canteros, B. I.; Proceedings of 9<sup>th</sup> International Conference of Plant Pathogenic Bacteria; Madras, Índia, 1996, p. 455.
7. Das, A. K.; *J. Appl. Hort.* **2003**, 5, 52.
8. Meneguim, L.; Rinaldi, D. A. M. F.; Santos, A. C. A.; Rodrigues, L. S.; Silva, M. R. L.; Canteri, M. G.; Leite Jr., R. P.; *Fitopatol. Bras.* **2007**, 32, 247.
9. Gottwald, T.; Graham, J.; Schubert, T.; *Plant Health Progress* **2002**, doi: 10.1094/PHP-2002-0812-01-RV.
10. Alcantara, G. B.; Honda, N. K.; Ferreira, M. M. C.; Ferreira, A. G.; *Anal. Chim. Acta* **2007**, 595, 3.
11. Lião, L. M.; Choze, R.; Cavalcante, P. P. A.; Santos, S. C.; Ferri, P. H.; Ferreira, A. G.; *Quim. Nova* **2010**, 33, 634.
12. Schneider, B.; *Prog. Nucl. Magn. Reson. Spectrosc.* **2007**, 51, 155.
13. Weljie, A. M.; Newton, J.; Jiric, F. R.; Vogel, H.; *J. Anal. Chem.* **2008**, 80, 8956.
14. Al-Hashimi, H. M.; Patel, D. J.; *J. Biomol. NMR* **2002**, 22, 1.
15. Sacco, A.; Bolsi, I. N.; Massini, R.; Spraul, M.; Humpfer, E.; Ghelli, S.; *J. Agric. Food Chem.* **1998**, 46, 4242.
16. Garrod, S.; Holmes, E.; Humpfer, E.; Spraul, M.; *Bruker Reports* **1998**, 146, 18.
17. Broberg, A.; Kenne, L.; Pedersen, M.; *Planta* **1998**, 206, 300.
18. Defernez, M.; Colquhoun, I. J.; *Phytochemistry* **2002**, 62, 1009.
19. Del Campo, G.; Berregi, I.; Caracena, R.; Santos, J. I.; Zhang, M.; *Anal. Chim. Acta.* **2006**, 556, 462.
20. Pérez, E. M. S.; Iglesias, M. J.; Ortiz, F. L.; Pérez, I. S.; Galera, M. M.; *Food Chem.* **2010**, 122, 877.
21. Correia, P. R. M.; Ferreira, M. M. C.; *Quim. Nova* **2007**, 30, 481.
22. Kuc, J.; *Eur. J. Plant Pathol.* **2001**, 107, 7.
23. Van Andel, O. M.; *Eur. J. Plant Pathol.* **1958**, 64, 307.
24. Li, W.; *Analyst* **2006**, 131, 777.
25. Le Gall, G.; Puaud, M.; Colquhoun, I. J.; *J. Agric. Food Chem.* **2001**, 49, 580.
26. Hammer, K. A.; Carson, C. F.; Riley, T. V.; *J. Appl. Microbiol.* **1999**, 86, 985.
27. Mishra, A. K.; Dubey, N. K.; *Appl. Environ. Microbiol.* **1994**, 60, 1101.
28. Cernadas, R. A.; Camillo, L. R.; Benedetti, C. E.; *Mol. Plant Pathol.* **2008**, 9, 609.
29. Fujikawa, T.; Ishihara, H.; Leach, J. E.; Tsuyumu, S.; *Mol. Plant-Microbe Interact.* **2006**, 19, 342.
30. Swarbrick, P. J.; Schulze-Lefert, P.; Scholes, J. D.; *Plant Cell Environ.* **2006**, 29, 1061.
31. Grennan, A. K.; *Plant Physiol.* **2007**, 144, 3.
32. Wilson, R. A.; Jenkinson, J. M.; Gibson, R. P.; Littlechild, J. A.; Wang, Z. Y.; Talbot, N.; *EMBO J.* **2007**, 26, 3673.

Submitted: November 5, 2011  
Published online: May 8, 2012

## <sup>1</sup>H HRMAS NMR Spectroscopy and Chemometrics for Evaluation of Metabolic Changes in *Citrus sinensis* Caused by *Xanthomonas axonopodis* pv. *citri*

Lorena M. A. Silva,<sup>a</sup> Elenilson G. Alves Filho,<sup>a</sup> Rafael Choze,<sup>a</sup> Luciano M. Lião<sup>a</sup> and Glauca B. Alcantara<sup>\*,a,b</sup>

<sup>a</sup>Laboratório de Ressonância Magnética Nuclear, Instituto de Química, Universidade Federal de Goiás, CP 131, 74001-970 Goiânia-GO, Brazil

<sup>b</sup>Departamento de Química, Centro de Ciências Exatas e Tecnologia, Universidade Federal de Mato Grosso do Sul, CP 549, 79074-460 Campo Grande-MS, Brazil

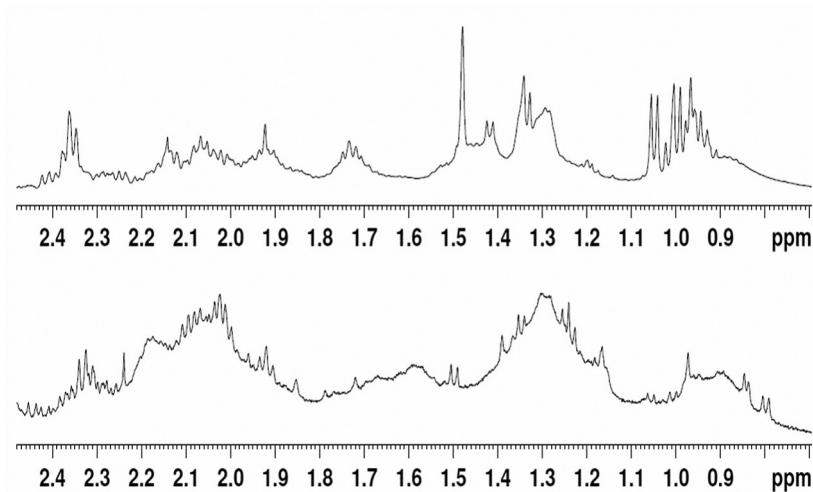


**Figure S1.** Comparative <sup>1</sup>H HRMAS NMR spectra from isolated *Xac* (above) and orange tree leaves with lesions caused by *Xac* (below).

\*e-mail: glauca.alcantara@ufms.br